Available online at www.sciencedirect.com
ScienceDirect
International Journal of Pharmaceutics 354 (2008) 180–195
INTERNATIONAL JOURNAL OF PHARMACEUTICS
www.elsevier.com/locate/ijpharm

Pharmaceutical Nanotechnology

Interaction of lipid nanoparticles with human epidermis and an organotypic cell culture model

Judith Kuntsche [a,b,*], Heike Bunjes [b,c], Alfred Fahr [b], Sari Pappinen [a], Seppo Rönkkö [a], Marjukka Suhonen [a], Arto Urtti [a,d]

[a] Department of Pharmaceutics, University of Kuopio, P.O. Box 1627, FIN-70211 Kuopio, Finland
[b] Department of Pharmaceutical Technology, Friedrich Schiller University Jena, Lessingstr. 8, D-07743 Jena, Germany
[c] Institute of Pharmaceutical Technology, Technical University Braunschweig, Mendelssohnstr. 1, D-38106 Braunschweig, Germany
[d] Drug Discovery and Development Technology Center, University of Helsinki, P.O. Box 56, FIN-00014 Helsinki, Finland

Received 21 June 2007; accepted 13 August 2007
Available online 25 August 2007

Abstract

Various lipid nanoparticle formulations were investigated with respect to (trans)dermal drug delivery with special regard to the mechanism of their effects on human and an organotypic cell culture epidermis. Potential alterations of stratum corneum lipid domains were studied using fluorescence assays with labeled liposomes and thermal analysis of isolated stratum corneum. Influences on the permeation of corticosterone were investigated and the occlusive properties of the nanoparticles were determined by measurements of the transepidermal water loss (TEWL). The penetration of a fluorescence dye was visualized by fluorescence microscopy of cross sections of human epidermis after incubation with cubic and solid lipid nanoparticles. Corticosterone permeation was limited when applied in matrix-type lipid nanoparticles (fat emulsion, smectic and solid lipid nanoparticles). An adhesion of solid lipid nanoparticles was clearly observed in thermal analysis as reflected by additional phase transitions probably caused by the nanoparticle matrix lipid. However, as for the other matrix-type nanoparticles, no distinct alterations of the phase transitions of the stratum corneum lipids were observed. Cubic nanoparticles led to the most predominant effect on skin permeation where the surface-active matrix lipid may act as penetration enhancer. An alteration of the stratum corneum lipids' thermal behavior as well as an interaction with fluorescence labeled liposomes was observed. Differences observed in permeation studies and thermal analysis of human and cell culture epidermis indicate that surface lipids, which are not present to the same extent in the cell culture model than in human epidermis, seem to play an important role.

Keywords: Colloidal drug carrier; (Trans)dermal drug delivery; Permeation; Stratum corneum thermal behavior; Organotypic cell culture

1. Introduction

Lipid nanoparticles are under investigation as drug carrier systems for poorly water soluble drugs especially with regard to parenteral administration (Klang and Benita, 1998; Müller et al., 2000; Westesen, 2000; Mehnert and Mäder, 2001). Moreover, these formulations – in particular solid lipid nanoparticles and the related nanostructured lipid carriers (Müller et al., 2002a,b; Jores et al., 2004) – are currently intensively studied with respect to (trans)dermal drug delivery.

Higher amounts of glucocorticoids in the upper skin were observed after 6 and 24 h when applied as solid lipid nanoparticle dispersions compared, e.g., to conventional creams and colloidal emulsions (Santos Maia et al., 2002; Sivaramakrishnan et al., 2004). For retinol-loaded solid lipid nanoparticles, the

Abbreviations: CM, cholesteryl myristate; CN, cholesteryl nonanoate; D116, tripalmitate; DSC, differential scanning calorimetry; FRET, fluorescence resonance energy transfer; GMO, glycerol monooleate; LD-PIDS, laser diffraction with polarization intensity differential scattering; MCT, medium chain triglycerides; PCS, photon correlation spectroscopy; PG, passage; POL, poloxamer; REK, rat epidermal keratinocytes; ROC, rat epidermal keratinocyte organotypic culture; SGC, sodium glycocholate; TEWL, transepidermal water loss; dpm, disintegrations per minute

* Corresponding author. Current address: Martin-Luther-University Halle-Wittenberg, Institute of Pharmacy, Department of Pharmaceutics and Biopharmaceutics, Wolfgang-Langenbeck-Str. 4, D-06120 Halle (Saale), Germany. Tel.: +49 345 5525210; fax: +49 345 5527029.
E-mail address: judith.kuntsche@pharmazie.uni-halle.de (J. Kuntsche).

0378-5173/$ – see front matter © 2007 Elsevier B.V. All rights reserved.
doi:10.1016/j.ijpharm.2007.08.028

drug amount in the upper skin was decreased considerably after a longer incubation time of 24 h compared to incubation for 6 h (Jenning et al., 2000a). This observation was attributed to a gel formation of the nanoparticle dispersion which may cause a pronounced occlusion as well as a change of the modification of the matrix lipid resulting in an expulsion of the drug from the nanoparticle matrix and a higher permeation rate (Jenning et al., 2000a,b). In some in vivo animal studies systemic effects were found after dermal administration of drug loaded colloidal fat emulsions (Friedmann et al., 1995; Schwarz et al., 1995) or solid lipid nanoparticles (Mei et al., 2003, 2005). For example, the application of anti-inflammatory drugs incorporated into colloidal lipid dispersions showed better effects compared to larger sized emulsions (Friedmann et al., 1995) or the drug solution (Mei et al., 2003) in the carrageenan paw edema model in rats. However, the anti-inflammatory effect was more pronounced when the formulation was applied at the site of inflammation, e.g., on the inflamed paw compared to an application on the back of the animals (Friedmann et al., 1995).

Besides for drug delivery to the skin, lipid nanoparticle dispersions – in particular solid lipid nanoparticles – seem to be promising formulations for cosmetics (Müller et al., 2002b; Wissing and Müller, 2003a) because of their positive influence on skin hydration and viscoelasticity (Wissing and Müller, 2003b; Üner et al., 2005) and their UV-blocking potential (Wissing and Müller, 2002).

Only little is, however, hitherto known about the mechanism of the lipid nanoparticle effects on drug transport into or through the skin as well as on drug retention in the different skin layers. Moreover, only few investigations compare the effect of different types of lipid nanoparticle formulations. The complexity of the colloidal systems (co-existence of different colloidal structures in the dispersions, potential polymorphism of solid lipid nanoparticles, etc.) complicates the situation.

In the present study, lipid nanoparticles differing in the state of their matrix lipid (isotropic liquid, liquid crystalline, solid crystalline) as well as the kind of the matrix lipid (non-polar, polar) were investigated. The majority of these nanoparticles [colloidal fat emulsion, supercooled smectic nanoparticles (Kuntsche et al., 2004; Bunjes and Kuntsche, 2007), solid lipid nanoparticles] consist of a continuous lipid matrix of non-polar lipids (triglycerides, cholesterol esters) stabilized, e.g., with a phospholipid-bile salt mixture. In contrast, cubic nanoparticles differ distinctly in their properties from these systems. The polar lipid glycerol monooleate forms a cubic lyotropic mesophase, which is stable in excess water so that colloidal dispersions can be prepared in the presence of stabilizers like poloxamer. Cubic nanoparticles are composed of hydrated glycerol monooleate bilayers separated by two intercrossing water channels (Wörle et al., 2006). They were included in this study because the polar character of the matrix lipid as well as the bilayered particle structure might be advantageous with respect to drug penetration and/or permeation (Bender et al., 2005; Esposito et al., 2005).

To get a deeper insight into the mechanism of the interaction of lipid nanoparticles with skin, the investigations were focused on:

- A possible alteration of lipid domains in the stratum corneum using fluorescence assays with labeled liposomes and thermal analysis of the stratum corneum after incubation with the respective formulations,
- the influence of the formulations on the transdermal permeation of the radiolabeled lipophilic model drug corticosterone,
- the occlusive properties of the nanoparticles as reflected in alterations of the transepidermal water loss (TEWL), and
- the penetration of a fluorescence dye visualized by fluorescence microscopy of cross sections of the epidermis after incubation with selected dispersions.

In addition to isolated human epidermis, an organotypic cell culture model was used. Reconstructed skin models are of particular interest as skin substitutes for e.g. large area burns (Boyce, 2001), for skin irritation testing of cosmetics or pharmaceuticals avoiding animal studies (Ponec, 2002; Pappinen et al., 2005) and studies on drug metabolism (Gysler et al., 1999). For investigations of drug penetration and permeation a competent barrier similar to the in vivo conditions is required. This is currently the main problem of many reconstructed skin models (Specht et al., 1998; Dreher et al., 2002; Schreiber et al., 2005; Netzlaff et al., 2007). For the organotypic cell culture model based on rat epidermal keratinocytes (REK) used in this study, a similar ultrastructure of the stratum corneum (Pasonen-Seppänen et al., 2001a,b) as for human skin and a comparable permeability for a large number of tested compounds could be established (Suhonen et al., 2003).

2. Material and methods

2.1. Materials

Medium chain triglycerides (MCT), tripalmitate (D116, Dynasan 116, both Hüls/Sasol, Germany), cholesteryl myristate (CM, ICN, USA), cholesteryl nonanoate (CN, Acros, USA), glycerol monooleate (GMOrphic-80, GMO, Eastman, USA), purified soybean phosphatidylcholine Lipoid S100 (Lipoid KG, Germany), poloxamer 407 (POL, Lutrol F127, BASF, Germany), sodium glycocholate (SGC), thiomersal, cholesterol, cholesterol sulfate, stearic acid, α-hydroxy fatty acid ceramides, non-hydroxy fatty acid ceramides, PBS buffer pH 7.40 tablets, TRIS base, boric acid (all from Sigma), glycerol (Solvay, Germany), [1,2,6,7-^{3}H(N)]-corticosterone (in ethanol, 37 MBq/ml, 2.6–3.7 TBq/mmol, Perkin Elmer), sodium bromide (Riedl-de-Haën/Sigma-Aldrich, Germany), calcein (Sigma), L-α-phosphatidylethanolamine-*N*-(lissamine rhodamine B sulfonyl) (N-Rh-PE, Avanti Polar Lipids, USA), 1,2-dioleolyl-*sn*-glycero-3-phosphatidylethanolamine-*N*-(7-nitro-2-1,3-benzoxadiazol-4-yl) (N-NBD-PE, Avanti Polar Lipids, USA), 1,1′-Dioctadecyl-3,3,3′3′-tetramethylindocarbocyanine perchlorate (DiI, Sigma). For the preparation of the dispersions, water for injection Ph.Eur. (prepared by subsequent filtration, deionization, reverse osmosis, and distillation) was used. For analytics and buffer preparation, purified water obtained by common laboratory water purification systems (prepared by deionization and filtration, Millipore, Germany) was used.

Table 1
Composition, homogenization conditions, storage temperatures of the dispersions and state of the nanoparticle matrices

	Matrix lipid(s)	Stabilizer(s)	Homogenization conditions	Storage temperature	State of the matrix lipid
Fat emulsion					
MCT	Medium chain triglycerides 10%	S100 4.0%, SGC 1.0%	600–620 bar, 34–36 °C, 5 min	4 °C	Isotropic liquid
Solid lipid nanoparticles					
D116	Tripalmitate 10%	S100 4.0%, SGC 1.0%	810–820 bar, 84 °C, 5 min	4 °C	Crystalline
Smectic nanoparticles					
CM/CN	Cholesteryl myristate 8%, cholesteryl nonanoate 2%	S100 4.0%, SGC 1.0%	980–1020 bar, 85–87 °C, 5 min	23–25 °C	Smectic (thermotropic) metastable
Cubic nanoparticles					
GMO	Glycerol monooleate 8.8%	POL 1.2%	370 bar, 40 °C, 15 min	23–25 °C	Cubic (lyotropic)

All concentrations are w/w and related to the whole dispersion prior to high-pressure homogenization. All dispersions were prepared with an aqueous phase containing 0.005% thiomersal for preservation and 2.5% glycerol for isotonization.

2.2. Preparation of the colloidal lipid dispersions

The colloidal lipid dispersions were prepared as described previously by high-pressure homogenization (Microfluidizer, Microfluidics Corp., USA) of a crude emulsion dispersed by Ultra-Turrax vortexing [matrix-type nanoparticles (Kuntsche et al., 2004)] or of an equilibrated cubic phase [cubic nanoparticles (Wörle et al., 2006)]. The composition, preparation and storage conditions are given in Table 1. For the preparation of the matrix-type nanoparticles, the stabilizers (phospholipid S100 and sodium glycocholate) were dispersed or dissolved in the water phase (about 24 h at room temperature) and the whole homogenization process was carried out at temperatures above the melting point of the matrix lipids for the lipids being solid at room temperature in the bulk phase (CM, CN, D116, Table 1). To obtain cubic nanoparticles, the glycerol monooleate was molten together with the poloxamer at around 70 °C. The homogeneous melt was dropped into the stirred water phase at room temperature. After equilibration for about 24 h at room temperature the crude emulsion was high-pressure homogenized. A part of the dispersion of cubic nanoparticles was autoclaved (Varioclav 65T, H + P Labortechnik AG, Germany) after homogenization.

For the preparation of DiI labeled dispersions, an appropriate volume of a stock solution of DiI in ethanol (2 mg/ml DiI) was pipetted into beakers to give a final concentration of 0.5 mg DiI per g matrix lipid(s). After evaporating the ethanol, the respective amount of lipids was added and the fluorescence dye was dissolved in the lipid melt. The dispersions were then prepared as described above. DiI labeled dispersions were used for investigations of the influence of the lipid nanoparticles on the thermal behavior of the stratum corneum, of the TEWL of the epidermis after incubation with the nanoparticle dispersions and for microscopic investigations.

Radiolabeled corticosterone used as model drug for permeation studies was incorporated into the colloidal dispersions by passive loading in trace amounts (1 μl drug stock solution per ml colloidal dispersion, 37 kBq/ml). The drug stock solution was pipetted into a Falcon tube and the solvent was allowed to evaporate. After addition of the colloidal dispersions, the formulations were shortly vortexed and equilibrated for about 24 h at room temperature under light protection. Prior to use, the dispersions were shortly vortexed again. The PBS solution of the radiolabeled drug was prepared accordingly using PBS buffer pH 7.4 instead of the colloidal dispersions.

2.3. Preparation of skin liposomes

The skin liposomes were prepared similarly as described by Kirjavainen et al. (1996) except that stearic acid was used instead of palmitic acid for practical reasons. Both fatty acids were found in the stratum corneum in comparable amounts (Schaefer and Redelmeier, 1996). The liposomes were composed of non-hydroxy fatty acid ceramides, α-hydroxy fatty acid ceramides, cholesterol, stearic acid and cholesterol-3-sulfate in a weight ratio of 25:15:25:25:10. Fifteen milligram of lipids were dissolved in chloroform/methanol (2:1, v/v) and the mixture was vacuum-dried under a stream of nitrogen using a rotary evaporator. For the preparation of liposomes for the fluorescence resonance energy transfer (FRET) assay appropriate volumes of stock solutions of N-Rh-PE and N-NBD-PE in chloroform (1 mg/ml) were added to the lipid solution to give a final concentration of the fluorescence dyes of each 1 mol% related to the lipids. Three milliliter PBS buffer pH 7.4 (137 mM sodium chloride, 10 mM phosphate buffer, 2.7 mM potassium chloride) or TRIS-borate buffer pH 9.0 (500 mM Tris, 140 mM boric acid) containing 70 mM calcein for the preparation of calcein entrapped liposomes, respectively, were added to the dried lipid film. The mixtures were hand-swirled for 30 min, sonicated (Sonorex Super RK 102H, Bandelin, Germany) under nitrogen atmosphere at 78–80 °C for 30 min and then allowed to equilibrate for 30 min at the same temperature. Non-trapped markers were removed by column chromatography on Sephadex G-50 gel equilibrated with PBS buffer pH 7.4. Since column purification dilutes the liposome dispersions, this procedure was done for both labeled skin liposome preparations. The dilution of the liposome dispersions upon column purification was estimated by measuring the count-rate of scattered light (PCS, Nicomp) which was around 1400–1500 Hz before and around 1000 Hz

after column purification for both dispersions (dilution of about 1.45).

2.4. Particle size measurements

2.4.1. Photon correlation spectroscopy (PCS)

Dynamic light scattering was measured at 25 °C and 173° with a ZetaSizer Nano (Malvern Instr., Germany) or 90° with a PSS Nicomp 380 ZLS (Nicomp, USA) after appropriately diluting the samples with purified water. The intensity weighted mean diameter (z-average diameter) and the polydispersity index (PDI) – an indication for the width of the particle size distribution – were determined using the instruments cumulant analysis software (ZetaSizer Nano). Since these parameters are not available by the Nicomp software, the mean particle size for these measurements is expressed as mean diameter by intensity assuming a log-normal size distribution ("Gaussian") as most basic approach. The particle size values given are the averages of 5–6 measurements over 5 min runs.

2.4.2. Laser diffraction with PIDS (LD-PIDS)

The combination of laser diffraction with PIDS (polarization intensity differential scattering) technology (LS 230 Particle Sizer, Beckman-Coulter, USA) theoretically allows measurements over a particle size range from about 40 nm up to 2000 μm. Data of laser diffraction and PIDS are combined to calculate the particle size distribution by the Coulter LS software. Samples were measured in purified water. The values given are the averages of 6–8 measurements over 90 s per run as the mean diameter and D99 value (diameter of the cumulative distribution at 99%) of the volume distribution.

2.5. Cryoelectron microscopy

A few microliters of diluted (cubic nanoparticles) or undiluted (skin liposomes) dispersion were placed on a holey grid (Quantifoil Micro Tools, Jena, Germany) and excess of liquid was removed with filter paper. The samples were cryofixed by rapid immersing into liquid ethane cooled to −170 °C to −180 °C in a cryobox (Carl Zeiss NTS GmbH, Oberkochen, Germany). Excess ethane was removed by blotting in the cold. The samples were transferred with a cryotransfer unit (Gatan 626-DH) into the pre-cooled cryoelectron microscope (Philips CM 120, Netherlands) operated at 120 kV and viewed under low dose conditions.

2.6. Small angle X-ray diffraction

Samples were measured with a Kratky camera (Hecus Braun X-ray systems, Austria) on a conventional X-ray source (copper anode FK 61-04 × 12) generator Iso-Debyeflex 3003 60 kV (Seifert-FPM, Freiberg, Germany) using a position sensitive detector (PSD-50M, M. Braun, Garching, Germany) over 30 (smectic nanoparticles) or 60 (cubic nanoparticles) min at 23 °C. The measured curves were desmeared and smoothed to obtain the diffractograms shown in Fig. 2.

2.7. Differential scanning calorimetry (DSC)

For DSC measurements a Pyris 1 and a DSC 7 (Perkin Elmer, USA) instrument was used. Approximately 8–15 mg of the dispersions were accurately weighed into 15-μl-standard aluminum pans (Perkin Elmer), heated above the melting temperature (isotropic melt) of the respective matrix lipid(s), cooled to −10 or −13 °C to crystallize the nanoparticles and heated up again with a scan rate of 5 °C/min. Separated and hydrated stratum corneum samples (see Sections 2.11 and 2.14) were punched into small pieces and about 3–6 mg were accurately weighted into 30-μl-standard aluminum pans (Perkin Elmer). The samples were heated to 100 °C, cooled to 0 °C and heated again to 100 °C with a scan rate of 10 °C/min. To achieve better baselines, most samples were cooled to 10 °C before the first heating run.

The respective empty standard aluminum pans were used as reference. Between all temperature scans, isothermal steps with duration of 300 s (dispersions) or 60 s (stratum corneum) were inserted. For better comparison, the DSC curves are normalized to a sample weight of 1 mg and shifted along the ordinate in the figures.

2.8. Fluorescence assays

Thirty microliter of labeled skin liposomes (FRET liposomes and calcein containing liposomes, respectively) and 5 ml PBS buffer pH 7.4 were mixed by manual shaking. Two hundred microliter of the diluted liposome dispersion were pipetted into the wells of 96 well plates and the initial fluorescence was measured. Two microliter of the diluted colloidal dispersions (1:10, v/v in PBS) were added to the labeled skin liposomes and mixed by up-and-down pipetting. The fluorescence (485 nm excitation and 535 nm emission) was then monitored for 30 min in a Victor^2 fluorescence well-plate reader (Perkin Elmer) at 37 °C. At the end of the measurement, the vesicles were disrupted by adding 5 μl of Triton X-100 solution (4%, w/v) and careful up-and-down pipetting. The values obtained in the presence of Triton X-100 were corrected for sample dilution and the effect of Triton X-100 (factor 1.67 for the calcein and 1.25 for the FRET assay). The resulting fluorescence level was set to 100% and the results are expressed as percentage of the maximum fluorescence. In some measurements, purified water was used instead of PBS buffer for dilution of the skin liposomes and the lipid dispersions.

2.9. Rat epidermal keratinocyte (REK) stock and rat epidermal keratinocytes organotypic culture (ROC)

The rat epidermal keratinocytes (REK) stock and organotypic cultures were cultivated as described earlier (Suhonen et al., 2003). In brief, stock cultures were grown in Minimum Essential Medium (MEM, Gibco BRL) supplemented with 10% fetal bovine serum (HyClone, USA), 4 mM L-glutamine, 100 U/ml penicillin and 100 μg/ml streptomycin (all from Sigma) at 37 °C in an atmosphere with 5% CO_2 and sub-cultured twice a week.

For the cultivation of the organotypic culture (ROC), recently confluent rat epidermal keratinocytes of different passage numbers were seeded out into collagen-coated inserts (Costar Transwell, diameter 24 mm, pore size of the polycarbonate membrane 3.0 μm) with a cell density of 400,000 cells/insert. The cultures were incubated (37 °C, 5% CO_2) with Dulbecco's Modified Eagle Medium (DMEM, high glucose and with L-glutamine, Gibco BRL) supplemented with 10% fetal bovine serum, 4 mM L-glutamine (final concentration 8 mM), 100 U/ml penicillin and 100 μg/ml streptomycin on the top and underneath the cells for 3 days. The culture medium was then removed from the surface of the cells and the cultures were further grown at the air–liquid interface for about 18 days using the supplemented DMEM containing additional 40 μg/ml Vitamin C (Sigma). Prior to use, the ROC epidermis was cut with the filter and collagen from the inserts. Due to high fragility of the ROC epidermis, filter and collagen were not removed for the experiments. The REK organotypic cultures (ROC) used for the experiments were obtained from stock keratinocyte cultures at passages 9–19.

2.10. Preparation of human epidermis

Human abdominal cadaver skin was obtained from the Kuopio University Hospital (Finland) with the permission from The National Board of Medicolegal Affairs. The excised skin was heated in purified water at 60 °C for 2 min and the epidermis was peeled off from the dermis, spread out and dried at room temperature under an air stream for about 2 days. The dried epidermis was cut into suitable pieces and frozen at −20 °C. Prior to use, the epidermis was allowed to thaw and hydrate by storage over PBS buffer pH 7.4 overnight at 4 °C. Epidermis from 6 different donors was used for the experiments.

2.11. Stratum corneum separation

The ROC or human epidermis was placed on a filter paper soaked with 0.1% (m/v) trypsin solution (trypsin type III from bovine pancreas, Sigma) in PBS pH 7.4 and stored at 4 °C for 24 h and afterwards at 37 °C for 1 h. The stratum corneum sheets were peeled off, shaken in 0.1% (w/v) trypsin inhibitor solution (trypsin inhibitor type II from soybean, Sigma) in purified water for about 30 s and then washed twice with purified water. The stratum corneum sheets were then placed onto a plastic grid, dried at room temperature and finally placed into a desiccator over silica gel in a nitrogen atmosphere and under light protection. Before use, the stratum corneum was hydrated over sodium bromide solution (27%, w/w) for about 48 h resulting in a hydration level of the stratum corneum of about 20% (Bouwstra et al., 1995).

2.12. Permeation studies

Franz diffusion chambers (Crown Glass Company, Somerville, USA) with a receptor volume of about 5 ml and an average effective area for diffusion of 0.64 cm^2 were used. The membranes were placed between the receptor and donor chamber with the stratum corneum side facing the donor compartment. Continuous magnetic stirring was maintained in the receptor chamber and the receptor fluid was thermostated at 37 °C. The Franz diffusion chambers were equilibrated for 30 min before placing the donor phase (0.5 ml) onto the epidermis. The donor compartments were covered with parafilm and aluminum foil. At pre-determined time intervals aliquots were withdrawn from the receptor chamber and replaced by the same volume of fresh buffer to maintain a constant volume. The permeation experiments were run over 47 h. The withdrawn samples were mixed with 3 ml of scintillation cocktail (UltimaGold, Packard, Bioscience, Netherlands) and analyzed by liquid scintillation counting (WinSpectral 1414, Wallac, Finland). After some experiments, the particle size of the dispersions was determined by PCS. The permeability coefficient P (cm/s) of the model drug was calculated at steady state under sink conditions according to Eq. (1):

$$P = \frac{1}{AC_D}\frac{dQ}{dt} \quad (1)$$

where A is the diffusional area of the diffusion cell (0.64 cm^2), C_D the concentration in the donor chamber (dpm/cm^3) and dQ/dt the slope of the linear region of the plot of the cumulative amount of corticosterone in the receptor chamber versus time (dpm/s). The linear range was between 22 and 47 h and the coefficients of linear regression were between 1.000 and 0.970, except for 2 measurements where these values were 0.944 and 0.932, respectively. Prior to the permeation studies, the integrity of the epidermis was checked by visual observation and TEWL measurements (OECD No. 28, 2004).

2.13. Dialysis experiments

For an approximation of the amount of corticosterone in the water phase of the colloidal dispersions, diffusion experiments with a dialysis membrane (MWCO 12–14 kDa, Visking, Medical International, UK) were carried out with the same experimental setup as in skin permeation studies (Franz diffusion chambers, temperature of the receptor phase 37 °C, volume of the donor phase 0.5 ml, volume of the receptor phase about 5 ml, diffusional area 0.64 cm^2). The dialysis membranes were hydrated in PBS buffer pH 7.4 for about 15 min prior to use.

The dialysis data were fitted with the SAAM compartmental program (SAAM II, Software Applications for Kinetic Analysis, Version 1.2.1, Saam Institute, University of Washington). The models used are shown in Fig. 1. The dialysis constant obtained by fitting the data of the PBS solution ($k_{D,R}$ and $k_{R,D}$) was used to fit the data obtained for the colloidal dispersions. The ratio of the initial concentration of corticosterone in the nanoparticle matrix and in the water phase (compartments $Donor_{NP}$ and $Donor_{AP}$, respectively) were varied and the concentration ratio resulting in the best fit of the data was used for the estimation of the corticosterone concentration in the aqueous phase of the dispersions.

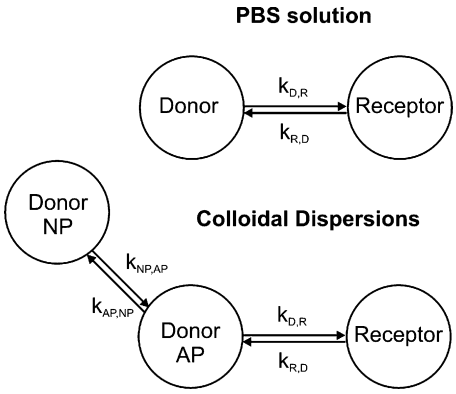

Fig. 1. Compartmental models used for fitting the dialysis data of corticosterone PBS solution and of the colloidal dispersions.

2.14. Measurements of the transepidermal water loss (TEWL)

The transepidermal water loss was measured using a VapoMeter with a closed measurement chamber [(Nuutinen et al., 2003), Delfin Technologies, Finland]. ROC or human epidermis was placed onto filter paper soaked with PBS. After removing excess of PBS and equilibration for 30 min at room temperature, the TEWL was measured for each epidermis in triplicate.

For the determination of the occlusive properties of the lipid nanoparticles, the initial TEWL value was measured as described above. Afterwards, an O-ring was placed onto the epidermis and weighted with a metal ring to avoid a leakage of the formulations. The epidermis was then incubated with 500 μl colloidal dispersions or with the aqueous phase of the dispersions (0.005% thiomersal and 2.5% glycerol, w/w), which served as control. The epidermis was covered throughout the incubation time with the formulations. DiI labeled nanoparticles were used for easier detection of possible leakages. After 24 h of incubation at room temperature and light protection, the formulations were carefully aspirated using an Eppendorf pipette. The membranes were rinsed with PBS by up and down pipetting using at least three times fresh PBS buffer and until the fluid appeared clear and no residues of the formulations onto the epidermis were detectable by visual observation. The TEWL was then determined after equilibration of the membranes for 30 min as described above. The occlusion factor was calculated according to Eq. (2):

$$\mathrm{OF} = \frac{\Delta\mathrm{TEWL_C}}{\Delta\mathrm{TEWL_D}} \quad (2)$$

where ΔTEWL is difference between the TEWL values after and before incubation of the control (C) and the colloidal dispersions (D), respectively. Afterwards the stratum corneum was separated and prepared for DSC measurements.

2.15. Light microscopic investigations

Human epidermis was incubated with the aqueous phase of the dispersions, solid and cubic nanoparticles labeled with DiI (0.5 mg DiI/g matrix lipid, 500 μl) for 24 h at 37 °C in Teflon chambers with PBS (preserved with thiomersal 0.005%, w/v) underneath the epidermis and under light protection. The epidermis was completely covered with the formulation throughout the incubation time. After incubation, the formulations were aspirated and the epidermis was extensively rinsed with water to remove all residues on the surface of the epidermis in order to avoid high fluorescence intensity on the top of the epidermis due to nanoparticle adhesion. Cross sections with a thickness of 5 μm were obtained by cutting the epidermis in a cryo-microtome (Leica CM 3050S, Leica Microsystems, Germany). The samples were then investigated by light microscopy (Olympus BX 40, Switzerland) in bright field and fluorescence mode (extinction 546 nm, emission 590 nm) with 400-fold magnification.

3. Results

3.1. Physicochemical properties and stability of the lipid nanoparticles

The particle size of the dispersions of the non-polar lipids with a continuous lipid matrix was around 100 nm. In contrast, a larger mean particle size of about 400 nm was obtained for the dispersions of cubic nanoparticles (Table 2).

The physical state of the solid and liquid crystalline matrix-type nanoparticles was confirmed by DSC and/or X-ray measurements (Fig. 2). The absence of a melting transition upon heating of the CM/CN nanoparticles in DSC as well as the characteristic X-ray reflection in the small angle range indicate the supercooled smectic state of these nanoparticles (Kuntsche et al., 2004). In contrast, a melting transition was observed already in the first DSC heating run for the D116 nanoparticles indicating their crystalline state (Bunjes et al., 1996).

Dispersions of cubic nanoparticles are usually prepared with a concentration of the dispersed phase (lipid and stabilizer) of 5% (Gustafsson et al., 1997; Wörle et al., 2006). For better comparison with the other colloidal dispersions of the present study which all contain 10% matrix lipid(s), a higher concentrated dispersion of cubic nanoparticles was, however, prepared (8.8% GMO and 1.2% poloxamer). For 5% systems with the same lipid/stabilizer ratio, a final autoclaving step is required for the formation of cubic particles from vesicular structures, which are predominant in the dispersions after high-pressure homogenization (Wörle et al., 2006). In contrast, a cubic particle structure was obtained for the 10% system already after high-pressure homogenization in the present investigation and autoclaving of this dispersion led to phase separation. Non-autoclaved dispersions were, therefore, used in the present study. The cubic state of the nanoparticles was confirmed by the occurrence of characteristic cubic reflections in small angle X-ray diffraction (Fig. 2) and the detection of mainly cubic particles in an electron microscopic investigation (Fig. 3A and B). Less ordered colloidal particles as well as vesicles were, however, observed beside the particles of cubic structure. The relatively large particle size of around 400 nm is in good agreement with the data obtained for the 5% systems after autoclaving (Wörle et al., 2006).

Table 2
Particle size of the dispersions after preparation, after storage and after a permeation study

	After preparation				After permeation study	After storage for about				
	PCS[a]		LD-PIDS		PCS[b]	2 months	≥15 months			
	z-average (nm)	PDI	Mean (nm)	D99 (nm)	Mean (by intensity) (nm)	PCS[b] Mean (by intensity) (nm)	PCS[a] z-average (nm)	PDI	LD-PIDS Mean (nm)	D99 (nm)
Fat emulsion										
MCT	121	0.15	113	413	118	123	122	0.15	110	404
Solid lipid nanoparticles										
D116	94	0.20	105	409	110	109	95	0.21	103	402
Smectic nanoparticles										
CM/CN	106	0.13	104	400	102	103	106	0.16	108	398
Cubic nanoparticles										
GMO	361	0.29	415	758	446	383	335	0.37	392	707

[a] ZetaSizer Nano.
[b] Nicomp Particle Sizer.

The incorporation of the fluorescence probe DiI into the colloidal dispersions did not alter the physicochemical properties of the colloidal dispersions (comparable particle size, no alteration of phase behavior and/or X-ray pattern). Also the incorporation of the radiolabeled corticosterone in trace amounts did not affect the particle size of the dispersions. Even after a permeation study, no distinct changes of the mean particle size were measured (Table 2), except for the dispersion of cubic nanoparticles, which showed an increased mean particle size after the permeation study.

The dispersions were stable with respect to the macroscopic appearance, particle size (Table 2) and state of the lipid matrix over the period of investigation.

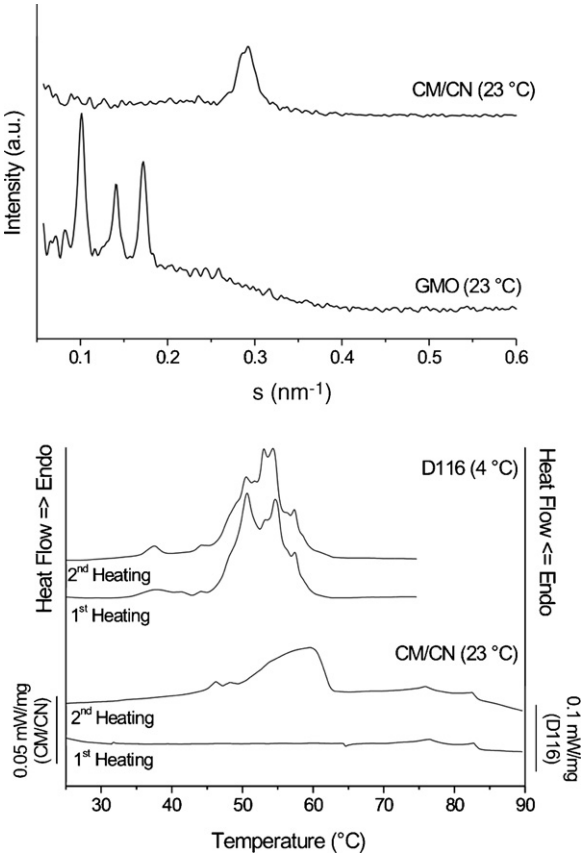

Fig. 2. Small angle X-ray (SAX) reflections of smectic and cubic nanoparticles (top) and DSC heating curves (5 °C/min) of solid and smectic nanoparticles (first and second heating run, bottom). The storage temperatures of the dispersions are given at the graphs. The measurements were carried out a few days after preparation of the dispersions. The reciprocal of the s-value (x-axis in the upper graph) corresponds to the d-spacing.

3.2. Interaction with fluorescence labeled skin liposomes

For the prediction of a possible permeation enhancement due to a disturbance of intercellular lipid domains of the stratum corneum, fluorescence assays using fluorescence labeled "skin liposomes" which contain lipids commonly found in the stratum corneum (Wertz et al., 1986; Schaefer and Redelmeier, 1996), can give a first insight (Kirjavainen et al., 1996). In the present study the calcein-release assay, where the fluorescence dye is located in a self-quenched concentration in the aqueous core of the liposomes, and the fluorescence resonance energy transfer (FRET) assay, where a matched pair of lipid probes (N-NBD-PE and N-Rh-PE as donor and acceptor, respectively) is located in the liposome bilayer, was used. In both assays a disturbance of the liposome membrane results in an increase in fluorescence intensity.

The mean particle size (PCS, Nicomp) of the calcein-loaded liposomes was comparable to the size of the unloaded, empty skin liposomes (about 125 nm), whereas the FRET liposomes had a slightly larger size (around 145 nm). In the cryoelectron microscopic investigations, all skin liposome dispersions appeared heterogeneous with respect to vesicle morphology (Fig. 3C–F). In particular in the FRET liposome dispersion a larger number of oligolamellar vesicles were detected (Fig. 3F).

Only cubic nanoparticles caused a strong increase in fluorescence intensity in the calcein-release and FRET assay (Fig. 4),

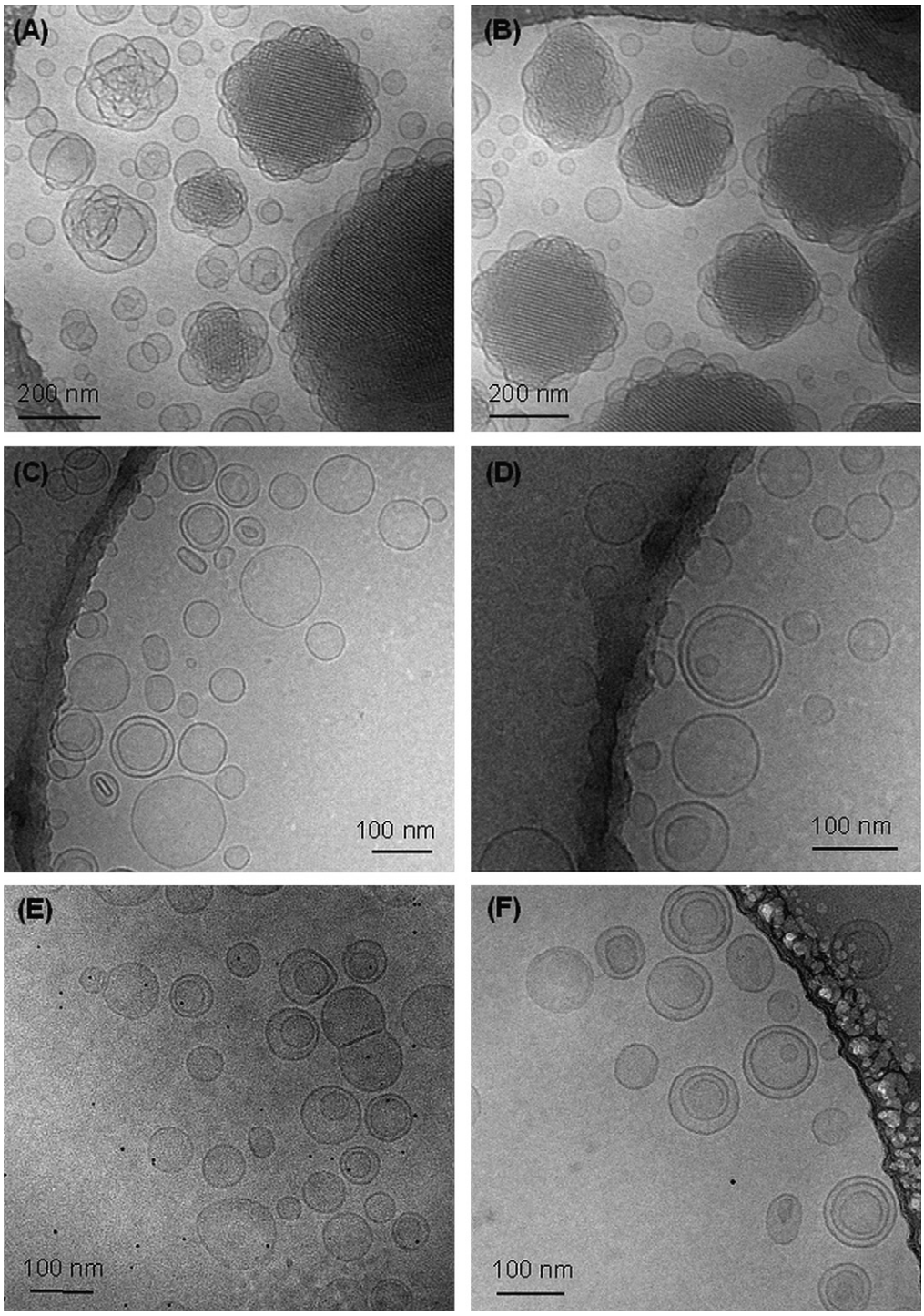

Fig. 3. Cryoelectron microscopic images of cubic nanoparticles and skin liposomes. (A and B) Cubic nanoparticles, (C and D) empty skin liposomes, (E) calcein-loaded skin liposomes and (F) FRET skin liposomes. The dark spots in (E) are probably caused by a contamination with ethane.

whereas the other lipid nanoparticles as well as empty skin liposomes, which were used as control, did not clearly interact with the labeled skin liposomes except for the solid lipid nanoparticles (D116) which surprisingly caused a distinct increase in fluorescence intensity in the FRET assay (Fig. 4). Since there was, however, no increase in fluorescence intensity in the calcein-release assay with these nanoparticles (Fig. 4), the effect in the FRET assay is probably not related to a direct interaction of the lipid nanoparticles with the skin liposomes. Dilution of the solid D116-nanoparticles in PBS buffer resulted in a slight but steady increase of the mean particle size with time indicating an aggregation of the nanoparticles. The intensity weighted mean diameter (PCS, Nicomp) was 111 nm after 5 min and 151 nm after 60 min, respectively. When the FRET assay was carried out in purified water (where the particles are stable), no distinct change in the fluorescence intensity was observed (Fig. 4)

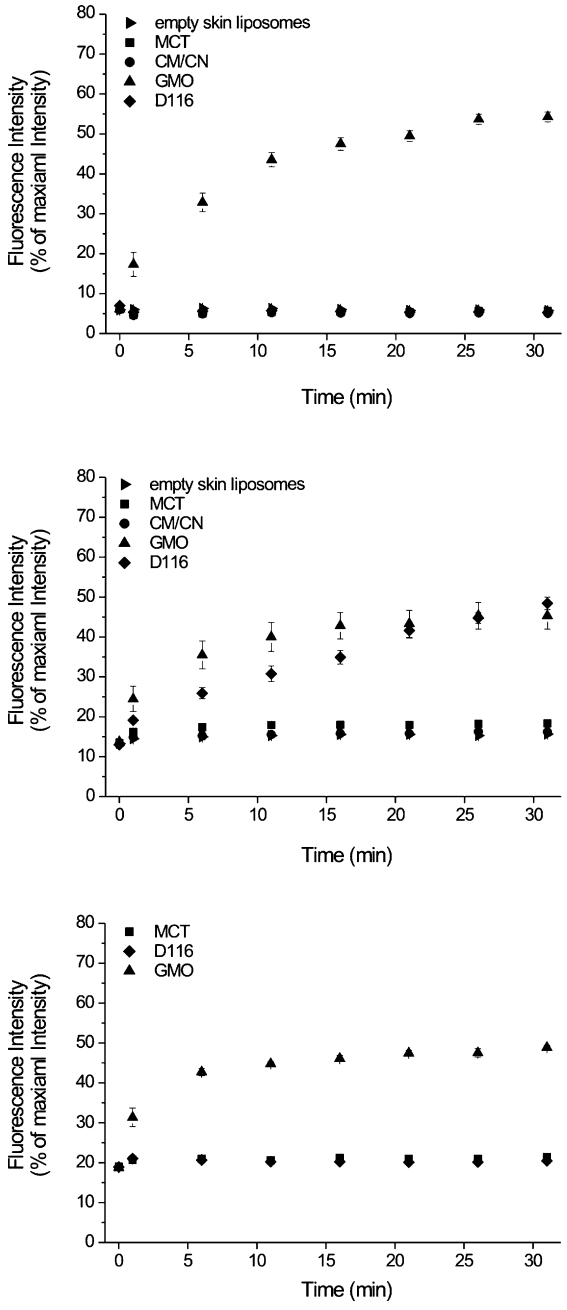

Fig. 4. Results of the fluorescence assays. Top: Calcein-release assay, middle: FRET assay measured in PBS buffer, bottom: FRET assay measured in purified water. Each data point represents the average of 8 values ± standard deviation.

indicating that the effect observed in the FRET assay measured in PBS is probably caused by an instability and aggregation of the tripalmitate nanoparticles and release and redistribution of at least one of the fluorescence probes into other colloidal structures or interfaces.

3.3. Permeation studies

The permeation of the model drug corticosterone was studied in dependence on the applied formulation (different colloidal lipid dispersions, PBS solution) using Franz diffusion chambers. In agreement with earlier results (Suhonen et al., 2003), corticosterone permeation from the PBS solution was about 2–3-fold higher in the ROC model than in human epidermis.

The application of the drug in colloidal lipid dispersions led to a strongly restricted permeation of the model drug through human epidermis, except for cubic nanoparticles for which permeation was only slightly lower compared to the PBS solution (Figs. 5 and 6). For the colloidal fat emulsion and solid lipid nanoparticles the observed corticosterone permeation was nearly negligible. In the ROC model corticosterone permeation was distinctly lower than from the PBS solution for all lipid nanoparticles applied (Figs. 5 and 6).

To obtain a first estimate of the drug content in the aqueous phase being available for free diffusion, dialysis experiments were carried out with the colloidal dispersions and the PBS solution. The cumulative amount of corticosterone in the receptor compartment in the dialysis experiments with the colloidal dispersions (Fig. 7) is a function of the dialysis constant (Washington, 1989), the release of corticosterone from the nanoparticles and the initial concentration of the drug in the aqueous phase of the dispersions. By fitting the dialysis data varying the ratio of the drug in the nanoparticle matrix and the aqueous phase of the dispersions and determining the qualities of the data-fits, the following amounts of corticosterone in the water phase of the dispersions were estimated: 9% for the solid lipid nanoparticles, 12% for the cubic nanoparticles, 16% for the fat emulsion and 24% for the smectic nanoparticles (Fig. 8).

Considering only the drug present in the water phase of the dispersions (correction of the donor concentration by the values obtained in the dialysis experiments) no influence of the nanoparticles with a continuous lipid matrix (fat emulsion, solid and smectic nanoparticles) on drug permeation was found in the ROC model, for cubic nanoparticles corticosterone permeation was, however, enhanced 2.4-fold compared to the PBS solution (Fig. 6). In human skin, drug permeation was reduced when applying the fat emulsion and solid lipid nanoparticles which both contain triglycerides as matrix lipids. Smectic nanoparticles seem to have no influence on the corticosterone permeation and similar results were obtained for human and the cell culture epidermis. Only cubic nanoparticles enhanced drug permeation distinctly and the enhancing effect was higher in human epidermis (7.0fold) than in the ROC culture (Fig. 6). However, the variation of the permeability coefficients was very high in human skin for smectic and cubic nanoparticles in particular between the skin samples obtained from different donors. Because the permeation profiles were very similar in all cases, all data were used for evaluation.

3.4. Influence of the colloidal dispersions on the phase behavior of the stratum corneum lipids

The thermal behavior of human and ROC stratum corneum differed distinctly (Fig. 9). For human stratum corneum transitions at about 36–38 °C, 72–74 °C and 85–86 °C (first heating run), usually referred to T_1, T_2 and T_3, were observed (Table 3) and are in reasonable agreement with literature data (Van Duzee, 1975; Golden et al., 1986; Gay et al., 1994; Cornwell et al., 1996;

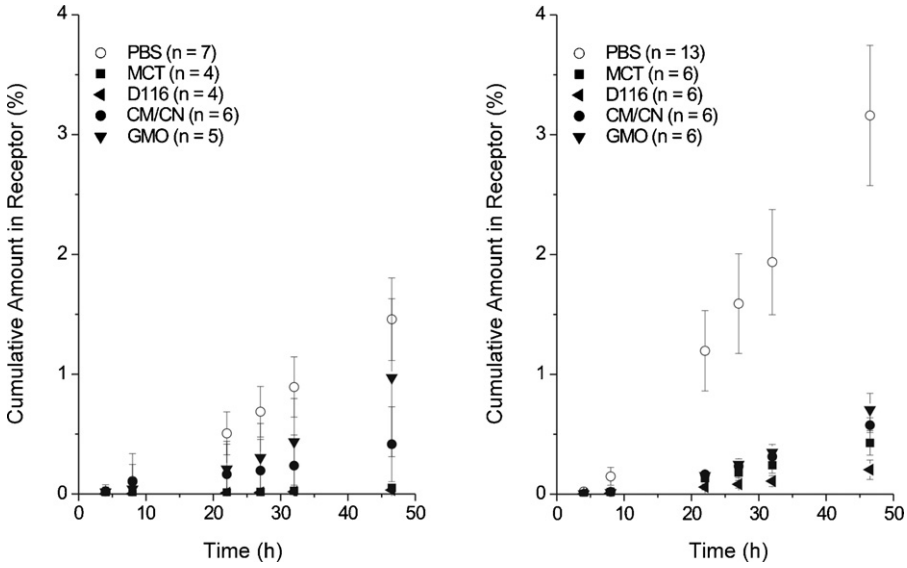

Fig. 5. Cumulative amount of corticosterone in the receptor compartment in the permeation studies with human (left) and ROC (right) epidermis in dependence on the applied formulation.

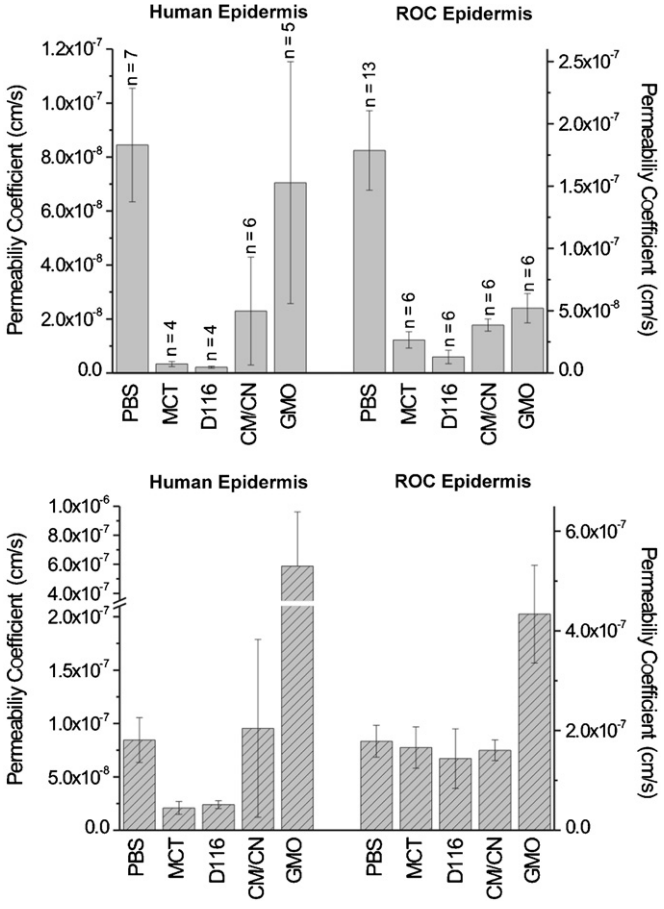

Fig. 6. Corticosterone permeability coefficients in dependence on the applied formulation in human and ROC epidermis. In the lower graph the donor concentrations were corrected to the estimated amount of free drug in the water phase of the dispersions. Note the different scales for ROC and human epidermis.

Al-Saidan et al., 1998). A further transition at around 50–55 °C (T_x) is described in the literature (Cornwell et al., 1996; Al-Saidan et al., 1998), but does not seem to occur in all cases (Van Duzee, 1975; Golden et al., 1986; Gay et al., 1994) and was neither detectable in the present study. Except for the low temperature transition (T_1) all transitions were reversible in human stratum corneum upon cooling and reheating. In ROC stratum corneum only one reversible transition at around 64–65 °C (first heating run) occurred which probably corresponds to the phase transition of intercellular lipids (T_2). The absence of the T_1 and T_3 transitions as well as the slightly lower T_2 transition compared to native rat stratum corneum (Al-Saidan et al., 1998; Al-Saidan, 2004) indicate some structural differences in the cell culture stratum corneum and might be responsible for an alteration of the barrier function.

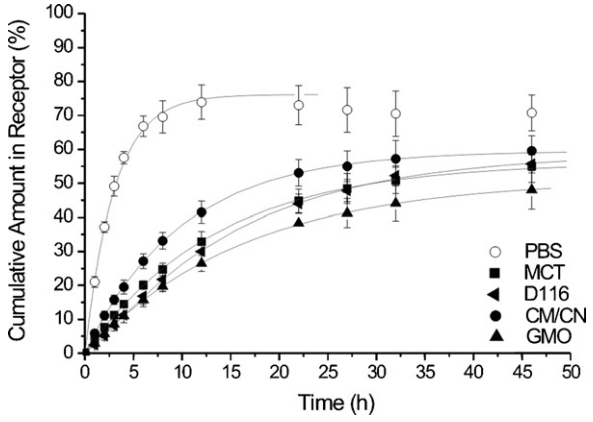

Fig. 7. Cumulative amount of corticosterone in the receptor compartment (symbols) in the dialysis experiments ($n = 5$–6) and the fits obtained by SAAM compartmental program (lines) assuming the following initial concentrations of corticosterone in the aqueous phase of the colloidal dispersions: 9% D116, 12% GMO, 16% MCT and 24% CM/CN.

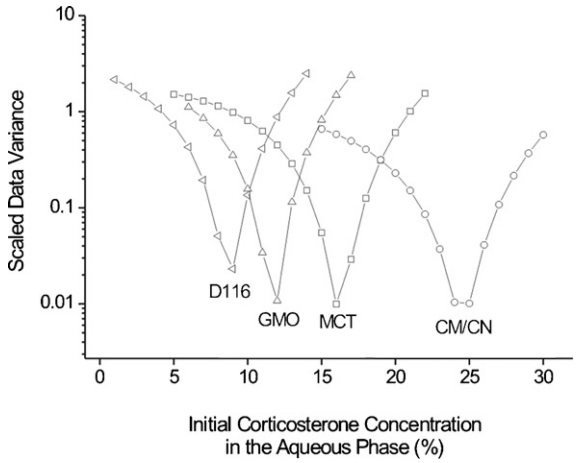

Fig. 8. Quality of the data-fits of the dialysis data in dependence on the initial concentration of corticosterone in the aqueous phase of the dispersions. For fitting the data of the dispersions, the dialysis constant obtained for the PBS solution was used.

The treatment of the membranes with the colloidal fat emulsion, smectic and solid lipid nanoparticles did alter the thermal behavior of neither human nor ROC stratum corneum distinctly (Table 3). Additional transitions were observed after incubation with solid lipid nanoparticles (Fig. 9) which are probably caused by the nanoparticle matrix lipid tripalmitate. The additional phase transitions of the ROC stratum corneum incubated with solid lipid nanoparticles occurred at about 58–59 °C and 43–44 °C in the first and second heating run, respectively, and are thus close to the melting temperatures of the β- (mp about 64 °C) and α-modification (mp about 45 °C) of tripalmitate in the bulk phase (Bunjes et al., 1996). In human stratum corneum the additional transitions were broader and shifted to lower temperatures (52 °C and 25–27 °C in the first and second heating run, respectively), which might be caused by mixing of tripalmitate with lipids present on the skin surface. In both human and ROC stratum corneum also an exothermic transition was observed in the cooling runs which can probably be attributed to triglyceride crystallization. Since there was no distinct alteration of the phase transitions of the stratum corneum lipids even in the second heating run, it is likely that the nanoparticles adhere to

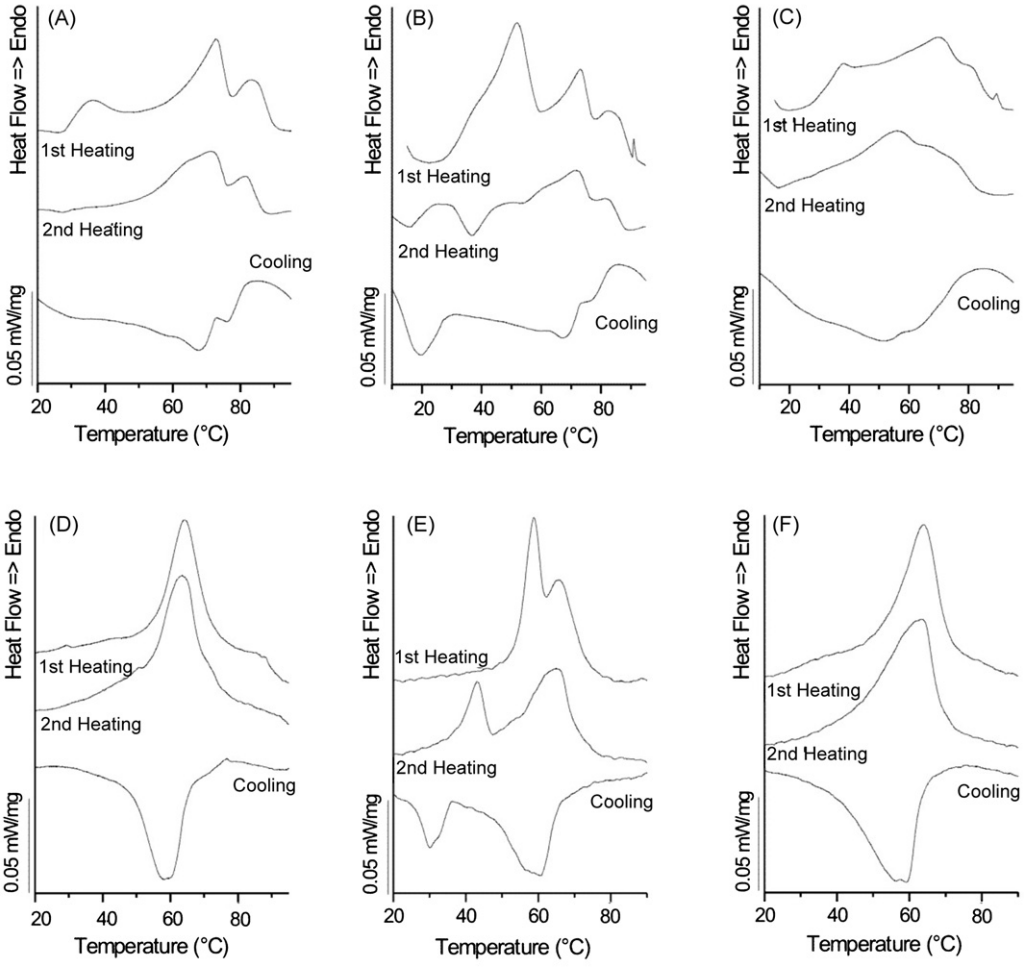

Fig. 9. DSC heating and cooling curves (10 °C/min) for human (A–C) and ROC (D–F) stratum corneum samples. A and D: controls, incubation with the aqueous phase of the dispersions, B and E: incubation with solid lipid nanoparticles (D116), C and F: incubation with cubic nanoparticles (GMO).

Table 3
Phase transition temperatures (peak temperatures) of the stratum corneum samples in dependence on treatment

	Human stratum corneum			ROC stratum corneum
	T_1	T_2	T_3	T_2
First heating				
Untreated	37.7 ± 0.2	73.8 ± 0.1	85.2 ± 0.8	63.9 ± 0.4
Control (AP)	36.7 ± 1.5	73.4 ± 0.9	85.2 ± 0.5	64.1 ± 0.2
Fat emulsion (MCT)	37.4 ± 0.5	73.8 ± 0.5	86.4 ± 1.2	64.7 ± 0.2
Solid lipid nanoparticles (D116)	37.0 ± 0.5/(51.7 ± 0.1)	73.3 ± 0.5	85.9 ± 1.0	(58.8 ± 0.2)/65.1 ± 0.6
Smectic nanoparticles (CM/CN)	36.6 ± 0.8	72.4 ± 1.1	85.4 ± 0.4	64.1 ± 0.1
Cubic nanoparticles (GMO)	37.3 ± 0.6	70.8 ± 0.8	85.4 ± 2.9	64.1 ± 0.3
Second heating				
Untreated		72.4 ± 0.1	82.6 ± 0.3	63.4 ± 0.6
Control (AP)		72.0 ± 2.2	83.5 ± 2.3	63.2 ± 0.3
Fat emulsion (MCT)		72.4 ± 1.1	83.8 ± 1.2	64.0 ± 0.1
Solid lipid nanoparticles (D116)	(26.34 ± 1.8)	72.1 ± 1.4	83.3 ± 1.2	(43.3 ± 0.3)/65.0 ± 0.3
Smectic nanoparticles (CM/CN)		71.3 ± 1.5	82.5 ± 0.9	63.5 ± 0.2
Cubic nanoparticles (GMO)		58.5 ± 9.3	74.7 ± 4.9	63.6 ± 0.2

The stratum corneum samples were incubated with the aqueous phase of the dispersions and the colloidal dispersions for 24 h at room temperature. The additional phase transitions after incubation with the solid lipid nanoparticles are set in parentheses. For comparison, untreated stratum corneum samples were measured as well (the human stratum corneum was isolated directly after the separation of the epidermis). Except for the untreated human stratum corneum ($n = 2$), the values given are the averages ± standard deviation of 3 samples.

the surface of the stratum corneum. In contrast to the original nanoparticle dispersion (Fig. 2), the stratum corneum samples did not display the multiple melting behavior typical for solid lipid nanoparticles of pure triglycerides (Unruh et al., 2001). This indicates an aggregation or fusion of the nanoparticles that may be induced or enforced by drying and preparation of the stratum corneum sheets for DSC measurements. After incubation with cubic nanoparticles the phase transitions of human stratum corneum were broadened and shifted to lower temperatures, particularly in the second heating runs. While in the first heating run only the transition attributed to the intercellular lipids (T_2) was shifted to lower temperatures, in the second heating run the T_3 transition was altered as well. The variation between the different samples (different donors) was, however, relatively high. In contrast to the situation with human stratum corneum the thermal behavior of the ROC model was only slightly influenced by cubic nanoparticles. The phase transition temperatures remained unchanged (Table 3) but the shape of the transition was altered and broadened, in particular during the second heating runs (Fig. 9) indicating a similar but weaker interaction with lipids of the stratum corneum as in human epidermis. The variation between the different samples was negligible in the ROC stratum corneum.

3.5. TEWL and occlusive properties of the nanoparticles

Non-invasive measurements of the transepidermal water loss (TEWL) are proposed for a fast evaluation of membrane integrity prior to other measurements like permeation studies (OECD No. 28, 2004). The TEWL is, however, relatively insensitive against small damages whereas already small damages of the stratum corneum may lead to a significantly increased drug permeation (Netzlaff et al., 2006). But since the measurement of the TEWL is non-invasive and a relatively fast method to obtain rough information about the barrier of the skin samples used, the TEWL was measured for most human skin samples and ROC membranes used in this study. The TEWL values of the ROC model were only slightly higher than those of human epidermis: the average TEWL was 10.7 ± 2.6 g/m^2 h ($n = 61$) and 13.4 ± 2.8 g/m^2 h ($n = 112$) for human and ROC epidermis, respectively.

The occlusive properties of the nanoparticles were determined by measurements of the TEWL before and after incubation with the formulations and the aqueous phase of the dispersion, which served as control (Fig. 10). Due to complete hydration during the whole incubation time, elevated TEWL values were measured after incubation in all samples, but the differences between the TEWL before and after incubation differed. The smaller the difference, the higher the occlusion effect caused by the lipid nanoparticles due to, e.g., an adhesion of the nanoparticles on the stratum corneum.

All lipid nanoparticles with a continuous matrix caused a small occlusion effect in human skin in the order: solid lipid

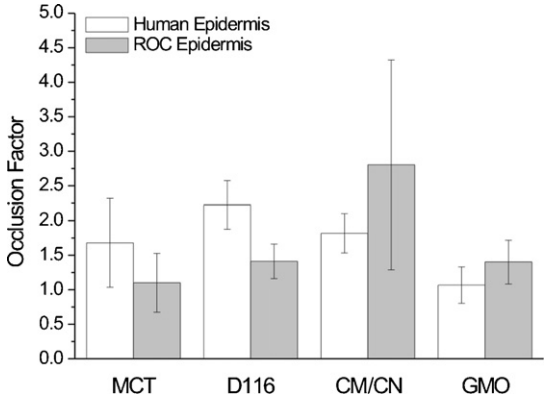

Fig. 10. Occlusion effect of the different lipid nanoparticles in human and ROC epidermis ($n = 3$–4).

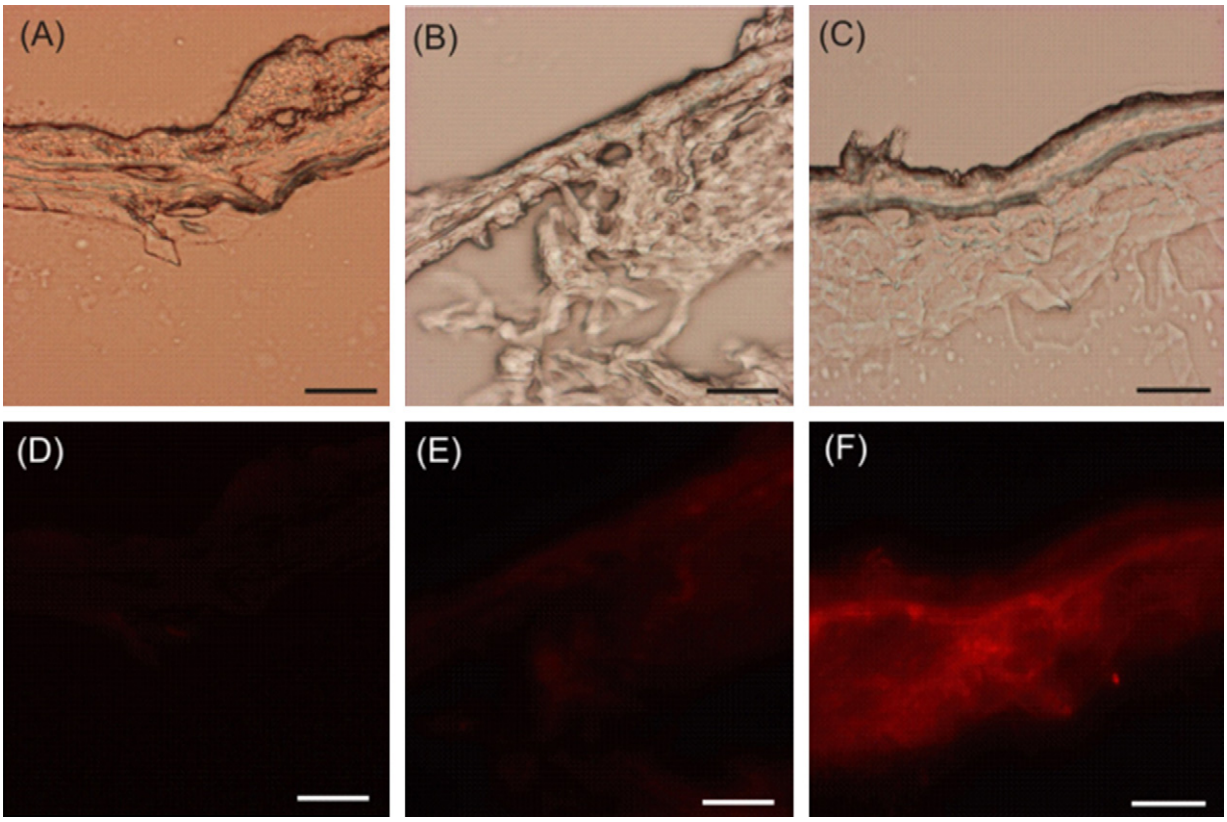

Fig. 11. Light (A–C) and fluorescence (D–F) microscopic images of cross sections of human epidermis incubated with the aqueous phase (control, without DiI, A and D), solid lipid nanoparticles (D116, B and E) and cubic nanoparticles (GMO, C and F). Bars = 20 μm.

nanoparticles > smectic nanoparticles > fat emulsion; the differences between the formulations were, however, only small. For cubic nanoparticles no effect was observed in human skin. In the ROC model, the occlusion effect of the solid lipid nanoparticles and the fat emulsion was lower than in human skin. For hitherto unclear reasons, smectic nanoparticles caused a relative high occlusion in ROC, but the variations between the single measurements were very high. For cubic nanoparticles a small occlusion effect was observed in the ROC model.

3.6. Fluorescence microscopy

To get information about the penetration of a model fluorescence dye incorporated into lipid nanoparticles, human epidermis was incubated with solid lipid and cubic nanoparticles labeled with a fluorescence dye (DiI, Fig. 11). As control and for determination of the auto fluorescence of the skin, the epidermis was also incubated with the aqueous phase of the dispersions (without DiI). The epidermis incubated with cubic nanoparticles fluoresced much more than the epidermis incubated with solid lipid nanoparticles in agreement with the results obtained in the permeation studies. In both cases, the fluorescence was distributed throughout the epidermis (Fig. 11).

4. Discussion

Lipid nanoparticles and particularly solid lipid nanoparticles are intensively investigated with respect to dermal or even transdermal drug delivery. In the present study, different methods were used to get a deeper insight into the interaction of the nanoparticles with the skin.

Under the conditions used in this study (trace amount of the model drug, infinite dose conditions), corticosterone permeation was not enhanced or even reduced when applied in lipid nanoparticles with a continuous lipid matrix (fat emulsion, solid and smectic lipid nanoparticles). These results indicate that these nanoparticles do not actively transport the drug incorporated into their lipid matrix through the stratum corneum so that mainly the drug dissolved in the water phase of the dispersions can pass the epidermis. It should be mentioned, however, that corticosterone used as model drug with moderate lipophilicity in this study was incorporated into the dispersions in trace amounts. Under these conditions, corticosterone is freely soluble in all phases of the colloidal dispersions (e.g., the lipid nanoparticle matrix and aqueous phase), which is normally not the case, but allowed the direct comparison to an aqueous solution of the drug. However, it is conceivable that a higher drug load of the nanoparticle matrix would result in an increased driving force for partitioning of the drug from the nanoparticle matrix into the stratum corneum after, e.g., adhesion of the nanoparticles onto the skin surface. In this regard, the localization of the drug in the nanoparticles (in the matrix or in the interface) seems to be of special importance (Sivaramakrishnan et al., 2004; Lombardi et al., 2005).

Depending on measurement conditions, a more or less distinct occlusion effect of solid lipid nanoparticles is described in the literature (Jenning et al., 2000a; Wissing and Müller,

2003a). The occlusion depended, in particular, on the size and crystallinity of the particles (Wissing and Müller, 2003a) with smaller particles and high crystallinity leading to highest occlusion factors. Accordingly, a slightly higher occlusion was observed in human skin in the present study for the crystalline solid nanoparticles compared to the colloidal fat emulsion and smectic nanoparticles, all with a comparable mean particle size of around 100 nm. The highly anisometric platelet particle shape of crystalline triglyceride nanoparticles (Bunjes, 2005) may facilitate adhesion of the nanoparticles onto the skin surface and thus occlusion.

The results of the permeation and DSC studies differed distinctly in human skin and the ROC model (Figs. 6 and 9). The highly restricted corticosterone permeation in human skin might be caused by the adhesion of the nanoparticles onto the skin surface, fusion with lipids present on the surface of the epidermis and formation of an additional diffusion barrier for the drug dissolved in the water phase. Surface lipids seem to play an important role for the nanoparticle adhesion and, consequently, for the restricted drug permeation. Occlusion caused by the triglyceride nanoparticles (fat emulsion, solid lipid nanoparticles) was less pronounced in the cell culture model where surface lipids are not present, at least not to the same extent as in human skin. Beside physiological skin surface lipids [mostly hydrophobic lipids with a high amount of triglycerides (Greene et al., 1970)], a contamination of the skin surface with subcutaneous lipids can, however, not be excluded in this study and the importance of physiological surface lipids needs further evaluation. Interestingly, corticosterone permeation was nearly comparable in human and ROC epidermis when applied in a dispersion of smectic nanoparticles indicating that the surface lipids seem to be less important for this carrier system. The adhesion of solid lipid nanoparticles to the stratum corneum was clearly observed in DSC as reflected by additional phase transitions (Fig. 9) attributed to the nanoparticle matrix tripalmitate and the distinct shift and broadening of the additional transitions in human stratum corneum also point to a mixing of tripalmitate with other lipids, probably mainly triglycerides. The occlusion effects observed for the fat emulsion and smectic nanoparticles indicate a similar nanoparticle adhesion to the skin surface as for the tripalmitate nanoparticles. However, corresponding effects may not be observable in DSC because medium chain triglycerides have no phase transitions in this temperature range and the transition enthalpies of cholesterol esters are distinctly smaller than those of triglycerides and thus too small for detection.

Only cubic nanoparticles enhanced corticosterone permeation. Due to the relatively large size of cubic nanoparticles (~400 nm) a penetration of the intact nanoparticles into the stratum corneum is unlikely. The surface-active glycerol monooleate might, however, enter the stratum corneum and act as penetration enhancer (Lopes et al., 2005). Since drug permeation was higher in human epidermis than in the ROC model, surface lipids seem to be important for these nanoparticles as well. An interaction with stratum corneum lipids was clearly observed by DSC in human skin whereas the effect on the ROC stratum corneum phase transition was only minor.

Results of the fluorescence assays and preliminary fluorescence microscopic investigations are in good agreement with results of permeation studies and DSC measurements: Lipid nanoparticles with a continuous matrix did not cause a disturbance of the skin liposome bilayer and the fluorescence of human epidermis after incubation with DiI-labeled solid lipid nanoparticles was very weak. In contrast, cubic nanoparticles clearly disturbed the lipid bilayer of the skin liposomes and a distinctly higher fluorescence of the epidermis was observed in fluorescence microscopy.

In conclusion, lipid nanoparticles with a continuous matrix of non-polar lipids seem to act more passively by an adhesion onto the skin surface rather than to deliver their drug load actively into or through the skin. A potential advantage of nanoparticle adhesion onto the skin and therefore a possible depot formation remains to be investigated in greater detail. In contrast, the application of cubic nanoparticles led to an enhanced permeation of corticosterone in human epidermis probably caused by the penetration of the polar lipid monooleate into the stratum corneum; an alteration of the thermal behavior of the stratum corneum was clearly seen in DSC measurements. Since lipids on the skin surface seem to play an important role for the action of lipid nanoparticles and a contamination of the epidermis used in this work with subcutaneous lipids cannot be excluded, it remains to be investigated if physiological sebum lipids cause similar effects particularly for triglyceride and cubic lipid nanoparticles. The present study focused on the stratum corneum as barrier of drug permeation using human separated epidermis and a cell cultured epidermis as models. Considering nanoparticles for (trans)dermal drug delivery, skin appendages can, however, not be neglected. During the last years, in particular the hair follicles received increasing attention with respect to drug delivery and targeting (Meidan et al., 2005; Bernard et al., 1997). An accumulation of polymeric nano- and microparticles (Alvarez-Román et al., 2004) and recently also of solid lipid nanoparticles has been described in the literature (Münster et al., 2005). Due to the homogeneous structure of the stratum corneum and the lack of special structures present in human skin, like hair follicles, glands and sebum lipids, cell culture models might be useful for an estimation of the importance of such structures on drug permeation and effects of different formulations particularly in an early stage of evaluation.

Acknowledgement

The authors thank Frank Steiniger for support in the electron microscopic investigations and the European Commission for financial support via a Marie Curie Fellowship for J. Kuntsche.

References

Al-Saidan, S.M., 2004. Transdermal self-permeation enhancement of ibuprofen. J. Control. Rel. 100, 199–209.

Al-Saidan, S.M., Barry, B.W., Williams, A.C., 1998. Differential scanning calorimetry of human and animal stratum corneum membranes. Int. J. Pharm. 168, 17–22.

Alvarez-Román, R., Naik, A., Kalia, Y.N., Guy, R.H., Fessi, H., 2004. Skin penetration and distribution of polymeric nanoparticles. J. Control. Rel. 99, 53–62.

Bender, J., Ericson, M.B., Merclin, N., Iani, V., Rosén, A., Engström, S., Moan, J., 2005. Lipid cubic phases for improved topical drug delivery in photodynamic therapy. J. Control. Rel. 106, 350–360.

Bernard, E., Dubois, J.L., Wepierre, J., 1997. Importance of sebaceous glands in cutaneous penetration of an antiandrogen: target effect of liposomes. J. Pharm. Sci. 86, 573–578.

Bouwstra, J.A., Gooris, G.S., Bras, W., Downing, D.T., 1995. Lipid organization in pig stratum corneum. J. Lipid Res. 36, 685–695.

Boyce, S.T., 2001. Design principles for composition and performance of cultured skin substitutes. Burns 27, 523–533.

Bunjes, H., Westesen, K., Koch, M.H.J., 1996. Crystallization tendency and polymorphic transitions in triglyceride nanoparticles. Int. J. Pharm. 129, 159–173.

Bunjes, H., 2005. Characterization of solid lipid nano- and microparticles. In: Nastruzzi, C. (Ed.), Lipospheres in Drug Targets and Delivery. CRC Press, Boca Raton, pp. 41–66.

Bunjes, H., Kuntsche, J., 2007. Supercooled smectic nanoparticles. In: Thassu, D., Deleers, M., Pathak, Y. (Eds.), Nanoparticulate Drug Delivery Systems. Informa Health Care, New York, pp. 129–140.

Cornwell, P.A., Barry, B.W., Bouwstra, J.A., Gooris, G.S., 1996. Modes of action of terpene penetration enhancers in human skin; differential scanning calorimetry, small-angle X-ray diffraction and enhancer uptake studies. Int. J. Pharm. 127, 9–26.

Dreher, F., Fouchard, F., Patouillet, C., Andrian, M., Simonnet, J.T., Benech-Kieffer, F., 2002. Comparison of cutaneous bioavailability of cosmetic preparations containing caffeine or α-tocopherol applied on human skin models or human skin ex vivo at finite doses. Skin Pharmacol. Appl. Skin Physiol. 15, 40–58.

Esposito, E., Cortesi, R., Drechsler, M., Paccamiccio, L., Mariani, P., Contado, C., Stellin, E., Menegatti, E., Bonina, F., Puglia, C., 2005. Cubosome dispersions as delivery systems for percutaneous administration of indomethacin. Pharm. Res. 22, 2163–2173.

Friedmann, D.I., Schwarz, J.S., Weisspapir, M., 1995. Submicron emulsion vehicle for enhanced transdermal delivery of steroidal and nonsteroidal antiinflammatory drugs. J. Pharm. Sci. 84, 324–329.

Gay, C.L., Guy, R.H., Golden, G.M., Mak, V.H.W., Francoeur, M.L., 1994. Characterization of low-temperature (i.e. <65 °C) lipid transitions in human stratum corneum. J. Invest. Dermatol. 103, 233–239.

Golden, G.M., Guzek, D.B., Harris, R.R., McKie, J.E., Potts, R.O., 1986. Lipid thermotropic transitions in human stratum corneum. J. Invest. Dermatol. 86, 255–259.

Greene, R.S., Downing, D.T., Pochi, P.E., Strauss, J.S., 1970. Anatomical variation in the amount and composition of human skin surface lipid. J. Invest. Dermatol. 54, 240–247.

Gustafsson, J., Ljusberg-Wahren, H., Almgren, M., Larsson, K., 1997. Submicron particles of reversed lipid phases in water stabilized by a nonionic amphiphilic polymer. Langmuir 13, 6964–6971.

Gysler, A., Kleuser, B., Sippl, W., Lange, K., Korting, H.C., Höltje, H.D., Schäfer-Korting, M., 1999. Skin penetration and metabolism of topical glucocorticoids in reconstructed epidermis and in excised human skin. Pharm. Res. 16, 1386–1391.

Jenning, V., Gysler, A., Schäfer-Korting, M., Gohla, S.H., 2000a. Vitamin A loaded solid lipid nanoparticles for topical use: occlusive properties and drug targeting to the upper skin. Eur. J. Pharm. Biopharm. 49, 211–218.

Jenning, V., Schäfer-Korting, M., Gohla, S., 2000b. Vitamin A-loaded solid lipid nanoparticles for topical use: drug release properties. J. Control. Rel. 66, 115–126.

Jores, K., Mehnert, W., Drechsler, M., Bunjes, H., Johann, C., Mäder, K., 2004. Investigations on the structure of solid lipid nanoparticles (SNL) and oil-loaded solid lipid nanoparticles by photon correlation spectroscopy, field-flow fractionation and transmission electron microscopy. J. Control. Rel. 95, 217–227.

Kirjavainen, M., Urtti, A., Jääskeläinen, I., Suhonen, T.M., Paronen, P., Valjakka-Koskela, R., Kiesvaara, J., Mönkkönen, J., 1996. Interaction of liposomes with human skin in vitro—the influence of lipid composition and structure. Biochim. Biophys. Acta 1304, 179–189.

Klang, S., Benita, S., 1998. Design and evaluation of submicron emulsions as colloidal drug carriers for intravenous administration. In: Benita, S. (Ed.), Submicron Emulsions in Drug Targeting and Delivery. Harwood Academic Publ., Amsterdam, pp. 119–152.

Kuntsche, J., Westesen, K., Drechsler, M., Koch, M.H.J., Bunjes, H., 2004. Supercooled smectic nanoparticles: a potential novel carrier system for poorly water soluble drugs. Pharm. Res. 21, 1834–1843.

Lombardi Borgia, S., Regehly, M., Sivaramakrishnan, R., Mehnert, W., Korting, H.C., Danker, K., Röder, B., Kramer, K.D., Schäfer-Korting, M., 2005. Lipid nanoparticles for skin penetration enhancement – correlation to drug localization within the particle matrix as determined by fluorescence and parelectric spectroscopy. J. Control. Rel. 110, 151–163.

Lopes, L.B., Collett, J.H., Bentley, M.V., 2005. Topical delivery of cyclosporin A: an in vitro study using monoolein as a penetration enhancer. Eur. J. Pharm. Biopharm. 60, 25–30.

Mehnert, W., Mäder, K., 2001. Solid lipid nanoparticles—production, characterization and applications. Adv. Drug Del. Rev. 47, 165–196.

Mei, Z., Chen, H., Weng, T., Yang, Y., Yang, X., 2003. Solid lipid nanoparticle and microemulsion for topical delivery of triptolide. Eur. J. Pharm. Biopharm. 56, 189–196.

Mei, Z., Wu, Q., Hu, S., Li, X., Yang, X., 2005. Triptolide loaded solid lipid nanoparticle hydrogel for topical application. Drug Dev. Ind. Pharm. 31, 161–168.

Meidan, V.M., Bonner, M.C., Michniak, B.B., 2005. Transfollicular drug delivery—Is it a reality? Int. J. Pharm. 306, 1–14.

Müller, R.H., Mäder, K., Gohla, S., 2000. Solid lipid nanoparticles (SLN) for controlled drug delivery—a review of the state of the art. Eur. J. Pharm. Biopharm. 50, 161–177.

Müller, R.H., Radtke, M., Wissing, S.A., 2002a. Nanostructured lipid matrices for improved microencapsulation of drugs. Int. J. Pharm. 242, 121–128.

Müller, R.H., Radtke, M., Wissing, S.A., 2002b. Solid lipid nanoparticles (SLN) and nanostructured lipid carriers (NLC) in cosmetic and dermatological preparations. Adv. Drug Del. Rev. 54, S131–S155.

Münster, U., Nakamura, C., Haberland, A., Jores, K., Mehnert, W., Rummel, S., Schaller, M., Korting, H.C., Zouboulis, Ch.C., Blume-Peytavi, U., Schäfer-Korting, M., 2005. RU 58841-myristate – prodrug development for topical treatment of acne and androgenetic alopecia. Pharmzie 60, 8–12.

Netzlaff, F., Kostka, K.H., Lehr, C.M., Schaefer, U.F., 2006. TEWL measurements as a routine method for evaluating the integrity of epidermis sheets in static Franz type diffusion cells in vitro. Limitations shown by transport data testing. Eur. J. Pharm. Biopharm. 63, 44–50.

Netzlaff, F., Kaca, M., Bock, U., Haltner-Ukomadu, E., Meiers, P., Lehr, C.M., Schaefer, U.F., 2007. Permeability of the reconstructed human epidermis model Episkin® in comparison to various human skin preparations. Eur. J. Pharm. Biopharm. 66, 127–134.

Nuutinen, J., Alanen, E., Autio, P., Lahtinen, M.R., Harvima, I., Lahtinen, T., 2003. A closed unventilated chamber for the measurement of transepidermal water loss. Skin Res. Technol. 9, 85–89.

OECD, Guidance document for the conduct of skin absorption studies, Number 28, 2004, OECD series on testing and assessment.

Pappinen, S., Pasonen-Seppänen, S., Suhonen, M., Tammi, R., Urtti, A., 2005. Rat epidermal keratinocyte organotypic culture (ROC) as a model for chemically induced skin irritation testing. Toxicol. Appl. Pharmacol. 208, 233–241.

Pasonen-Seppänen, S., Suhonen, T.M., Kirjavainen, M., Miettinen, M., Urtti, A., Tammi, M., Tammi, R., 2001a. Formation of permeability barrier in epidermal organotypic culture for studies on drug transport. J. Invest. Dermatol. 117, 1322–1324.

Pasonen-Seppänen, S., Suhonen, T.M., Kirjavainen, M., Suihko, E., Urtti, A., Miettinen, M., Hyttinen, M., Tammi, M., Tammi, R., 2001b. Vitamin C enhances differentiation of a continuous keratinocyte cell line (REK) into epidermis with normal stratum corneum ultrastructure and functional permeability barrier. Histochem. Cell Biol. 116, 287–297.

Ponec, M., 2002. Skin constructs for replacement of skin tissues for in vitro testing. Adv. Drug Del. Rev. 54, S19–S30.

Santos Maia, C., Mehnert, W., Schaller, M., Korting, H.C., Gysler, A., Haberland, A., Schäfer-Korting, M., 2002. Drug targeting by solid lipid nanoparticles for dermal use. J. Drug Targ. 10, 489–495.

Schaefer, H., Redelmeier, T., 1996. Skin Barrier. Principles of Percutaneous Absorption. Karger Basel, pp. 43–86, chapter 2.

Schreiber, S., Mahmoud, A., Vuia, A., Rübbelke, M.K., Schmidt, E., Schaller, M., Kandárová, H., Haberland, A., Schäfer, U.F., Bock, U., Korting, H.C., Liebsch, M., Schäfer-Korting, M., 2005. Reconstructed epidermis versus human and animal skin in skin absorption studies. Toxicol. in Vitro 19, 813–822.

Schwarz, J.S., Weisspapir, M.R., Friedmann, D.I., 1995. Enhanced transdermal delivery of diazepam by submicron emulsion (SME) creams. Pharm. Res. 12, 687–692.

Sivaramakrishnan, R., Nakamura, C., Mehnert, W., Korting, H.C., Kramer, K.D., Schäfer-Korting, M., 2004. Glucocorticoid entrapment into lipid carriers – characterization by parelectric spectroscopy and influence on dermal uptake. J. Control. Rel. 97, 493–502.

Specht, Ch., Stoye, I., Müller-Goymann, C.C., 1998. Comparative investigations to evaluate the use of organotypic cultures of transformed and native dermal and epidermal cells for permeation studies. Eur. J. Pharm. Biopharm. 46, 273–278.

Suhonen, T.M., Pasonen-Seppänen, S., Kirjavainen, M., Tammi, M., Tammi, R., Urtti, A., 2003. Epidermal cell culture model derived from rat keratinocytes with permeability characteristics comparable to human cadaver skin. Eur. J. Pharm. Sci. 20, 107–113.

Üner, M., Wissing, S.A., Yener, G., Müller, R.H., 2005. Skin moisturizing effect and skin penetration of ascorbyl palmitate entrapped in solid lipid nanoparticles (SLN) and nanostructured lipid carriers (NLC) incorporated into hydrogel. Pharmazie 60, 751–755.

Unruh, T., Bunjes, H., Westesen, K., Koch, M.H.J., 2001. Investigations on the melting behavior of triglyceride nanoparticles. Colloid Polym. Sci. 279, 398–403.

Van Duzee, B.F., 1975. Thermal analysis of human stratum corneum. J. Invest. Dermatol. 65, 404–408.

Washington, C., 1989. Evaluation of non-sink dialysis methods for the measurement of drug release from colloids: effects of drug partition. Int. J. Pharm. 56, 71–74.

Wertz, P.W., Abraham, W., Landmann, L., Downing, D.T., 1986. Preparation of liposomes from stratum corneum lipids. J. Invest. Dermatol. 87, 582–584.

Westesen, K., 2000. Novel lipid-based colloidal dispersions as potential drug administration systems – expectations and reality. Colloid. Polym. Sci. 278, 608–618.

Wissing, S.A., Müller, R.H., 2002. The development of an improved carrier system for sunscreen formulations based on crystalline lipid nanoparticles. Int. J. Pharm. 242, 373–375.

Wissing, S.A., Müller, R.H., 2003a. Cosmetic applications for solid lipid nanoparticles (SLN). Int. J. Pharm. 254, 65–68.

Wissing, S.A., Müller, R.H., 2003b. The influence of solid lipid nanoparticles on skin hydration and viscoelasticity – in vivo study. Eur. J. Pharm. Biopharm. 56, 67–72.

Wörle, G., Siekmann, B., Koch, M.H.J., Bunjes, H., 2006. Transformation of vesicular into cubic nanoparticles by autoclaving of aqueous monoolein/poloxamer dispersions. Eur. J. Pharm. Sci. 27, 44–53.